

# PROCEEDINGS OF SPIE

[SPIDigitalLibrary.org/conference-proceedings-of-spie](https://spiedigitallibrary.org/conference-proceedings-of-spie)

## New excitation wavelengths for dysprosium-doped mid-infrared fiber lasers

Amin, M., Majewski, M., Woodward, R., Fuerbach, A., Jackson, S.

M. Z. Amin, M. R. Majewski, R. I. Woodward, A. Fuerbach, S. D. Jackson, "New excitation wavelengths for dysprosium-doped mid-infrared fiber lasers," Proc. SPIE 11260, Fiber Lasers XVII: Technology and Systems, 112601R (21 February 2020); doi: 10.1117/12.2547152

**SPIE.**

Event: SPIE LASE, 2020, San Francisco, California, United States

# New excitation wavelengths for dysprosium-doped mid-infrared fiber lasers

M. Z. Amin<sup>a</sup>, M. R. Majewski<sup>a</sup>, R. I. Woodward<sup>a</sup>, A. Fuerbach<sup>b</sup>, and S. D. Jackson<sup>a</sup>

<sup>a</sup>MQ Photonics, School of Engineering, Macquarie University, NSW 2109, Australia

<sup>b</sup>MQ Photonics, Department of Physics and Astronomy, Macquarie University, NSW 2109, Australia.

## ABSTRACT

Mid-infrared (mid-IR) fiber lasers that are based on dysprosium (Dy) as the active laser ion provide emission in the wavelength range between 2.6–3.4  $\mu\text{m}$  and can thus bridge the spectral gap between holmium (Ho) and erbium (Er) based mid-IR lasers. Another distinct feature is the wide choice of pump wavelengths (1.1  $\mu\text{m}$ , 1.3  $\mu\text{m}$ , 1.7  $\mu\text{m}$ , and 2.8  $\mu\text{m}$ ) that can be used. To date, pump wavelengths shorter than 1.1  $\mu\text{m}$  have not been reported and all demonstrated pump wavelengths apart from in-band pumping suffer from pump excited state absorption (ESA). In this paper, we report new excitation wavelengths, 0.8  $\mu\text{m}$  and 0.9  $\mu\text{m}$ , for Dy-doped mid-IR fiber lasers. We have measured 18.5% and 23.7% slope efficiency (relative to launched pump power) for 0.8  $\mu\text{m}$  and 0.9  $\mu\text{m}$  pumping wavelengths, respectively. By comparing the residual pump power of experimental and numerical simulation data of a 0.5 m Dy-doped fiber, we have found that these new excitation wavelengths are free from pump ESA. Moreover, the high power laser diodes are commercially available at these new excitation wavelengths; therefore, the realization of a diode-pumped Dy-doped mid-infrared fiber laser might become feasible in the near future.

**Keywords:** Dysprosium, mid-infrared, fiber laser, new excitation wavelengths, diode-pumped

## 1. INTRODUCTION

Rare-earth-doped mid-infrared (mid-IR) fiber lasers have a wide range of applications in spectroscopy, defence, sensing, polymer processing and medicine.<sup>1–6</sup> Improvement of the existing mid-IR sources and extension of accessible mid-IR lasing wavelength towards the longer wavelengths will enable new applications. Particularly, 3–5  $\mu\text{m}$  spectral range can be used in sensing and polymer processing by exploiting the inherent absorption features of several important molecular bonds such as C-H, C-O, and N-H. Moreover, the existence of the important atmospheric transmission window in this spectral band opens up the opportunities of laser countermeasures of heat-seeking missiles and light detection and ranging (LIDER) applications.<sup>3,7</sup>

To generate mid-IR emission for these applications, low phonon energy fluoride glass is chosen as the dopant host of the rare-earth ions. The most successful and common fluoride glass composition suitable for mid-IR emission is  $\text{ZrF}_4\text{-BaF}_2\text{-LaF}_3\text{-AlF}_3\text{-NaF}$  (ZBLAN). Until now, three dopant ions such as erbium (Er), holmium (Ho) and dysprosium (Dy) have been reported for mid-IR signal generation. The 2.6–2.95  $\mu\text{m}$  and 3.3–3.8  $\mu\text{m}$  spectral range emission have been reported from Er:ZBLAN fiber.<sup>8,9</sup> The 2.8–3.0  $\mu\text{m}$  spectral range has been reported from a Ho:ZBLAN fiber laser, pumped at 1.15  $\mu\text{m}$ .<sup>10</sup>

The third dopant Dy has significantly wider emission cross-section covering from 2.6–3.4  $\mu\text{m}$  and can fill up the intermediate spectral gap of Er and Ho. This ion has many closely spaced levels, which enables several excitation wavelengths for mid-IR laser emission. So far 1.1  $\mu\text{m}$ , 1.3  $\mu\text{m}$ , 1.7  $\mu\text{m}$  and 2.8  $\mu\text{m}$  excitation wavelengths have been reported for Dy-doped mid-IR fiber laser. In the first attempt of Dy-doped mid-IR fiber laser demonstration, 1.1  $\mu\text{m}$  pumping wavelength was used as an excitation source.<sup>11</sup> In that first demonstration, the maximum mid-IR laser output power of 275 mW was measured with 4.5% (with respect to absorbed pump power) slope efficiency. In the following demonstration using the same pumping wavelength, the laser slope efficiency was increased to 23% relative to absorbed pump power by using an optimized 50% output coupler.<sup>12</sup> The use of 1.3  $\mu\text{m}$  pumping

---

Send correspondence to md-ziul.amin1@students.mq.edu.au

wavelength reduces the quantum defect and therefore should increase the laser slope efficiency. However, a lower slope efficiency 20% (with respect to absorbed pump power) was measured for 1.3  $\mu\text{m}$  wavelength.<sup>13</sup> These low slope efficiencies were explained by the existence of a detrimental pump excited state absorption.

Recently, Dy-doped mid-IR fiber lasers have received significant interest for in-band pumping to exploit the benefit of the low quantum defect, which enables highly efficient Dy-doped fiber laser.<sup>14</sup> With the in-band 2.8  $\mu\text{m}$  pumping wavelength a record slope efficiency (73% with respect to launched pump power and 77% with respect to absorbed pump power) has been reported from a Dy-doped mid-IR fiber laser.<sup>15</sup> In another report, the Dy-doped mid-IR fiber laser output has been scaled up to 10.1 W with this in-band pumping wavelength.<sup>16</sup> Though the in-band pumping wavelength provides the highest slope efficiency, the full emission bandwidth of  $\sim 3 \mu\text{m}$  and beyond 4  $\mu\text{m}$  emission of a Dy ion can not be accessed. For the in-band pumping Dy-doped fiber lasers, pump and signal fall under the same gain bandwidth, which limits the shorter wavelength access of  ${}^6\text{H}_{13/2}$  to  ${}^6\text{H}_{15/2}$  transition.<sup>17</sup> Moreover,  ${}^6\text{H}_{11/2}$  to  ${}^6\text{H}_{13/2}$  transition of a Dy ion, which can generate beyond 4  $\mu\text{m}$  emission, is inaccessible with this in-band pumping wavelength. Therefore, re-investigation of near-infrared (near-IR) pumping wavelengths are required to access the full  $\sim 3 \mu\text{m}$  emission bandwidth and beyond 4  $\mu\text{m}$  emission from a Dy ion (as done in<sup>18</sup> and <sup>7</sup> with 1.7  $\mu\text{m}$  pumping wavelength). However, 1.7  $\mu\text{m}$  pumping wavelength is not free from detrimental pump ESA, which limits the laser slope efficiency to 21% (with respect to launched pump power).

In this paper, we report two new excitation wavelengths (0.8  $\mu\text{m}$  and 0.9  $\mu\text{m}$ ) which are conveniently available from cost-effective high power laser diodes. In addition, the Dy energy diagram includes large forbidden energy gap between the  ${}^4\text{F}_{9/2}$  and  ${}^6\text{F}_{3/2}$  level, (as shown in Figure 1.) and hence these new pump wavelengths should not exhibit any detrimental pump ESA. These new excitation wavelengths can excite the ground state Dy ions to either  ${}^6\text{F}_{5/2}$  state (energy  $\sim 12.5 \times 10^3 \text{ cm}^{-1}$  corresponds to 0.8  $\mu\text{m}$ ) or  ${}^6\text{F}_{7/2}$  state (energy  $\sim 11 \times 10^3 \text{ cm}^{-1}$  corresponds to 0.9  $\mu\text{m}$ ). From these excited states, Dy ions non-radiatively decay back to the meta-stable state  ${}^6\text{H}_{13/2}$  (energy  $\sim 3.5 \times 10^3 \text{ cm}^{-1}$ ) from where they decay back to the ground state producing  $\sim 3 \mu\text{m}$  emission. As there is no possible resonant pump absorption from the meta-stable state to any higher energy state for these new excitation wavelengths, these wavelengths should not excite the meta-stable ions to higher energy state and can avoid the detrimental pump ESA.

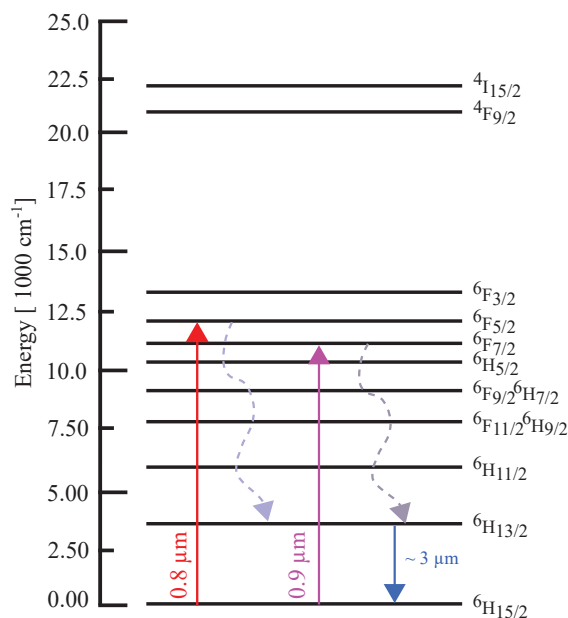


Figure 1. A simplified energy level diagram of a Dy ion. Existence of a large forbidden energy gap between the  ${}^4\text{F}_{9/2}$  and  ${}^6\text{F}_{3/2}$  level ensures no resonant pump absorption from the meta-stable state  ${}^6\text{H}_{13/2}$  to higher energy states.

## 2. EXPERIMENTAL SETUP

A simple linear cavity, as shown in Figure 2, is used to realise a 0.8  $\mu\text{m}$  and 0.9  $\mu\text{m}$  pumped Dy-doped mid-IR fiber laser. A single-clad Dy-doped ZBLAN fiber with 0.2 mol% doping concentration made by Le Verre Fluoré, France, is used as the laser gain medium. The Dy-doped fiber core diameter and numerical aperture are 12.5  $\mu\text{m}$ , 0.16, respectively, which ensure single mode operation down to 2.6  $\mu\text{m}$ . The Dy-doped fiber is either pumped at 0.8  $\mu\text{m}$  or 0.9  $\mu\text{m}$ , which is generated from a tunable titanium-sapphire laser (see the pump spectrum in Figure 3 (a)). The pump beam is focused into the Dy-doped fiber with 77% launching efficiency by using an anti-reflection coated aspheric lens of 12 mm focal length. In our experiment, two different Dy-doped fiber lengths (0.48 m and 0.62 m) have been used as the laser gain medium. To form the laser cavity two mirrors are butt-coupled at the end faces, which are perpendicularly cleaved, of the Dy-doped fiber. The butt-coupled mirror in the pumping end is partially transmissive (PT), 80% at 0.8  $\mu\text{m}$  and 73% at 0.9  $\mu\text{m}$ , for both pumping wavelengths and highly reflective (98%) from 2.7–3.2  $\mu\text{m}$ . The butt-coupled mirror in the far-end of the fiber is a 50% broad-band reflective mirror around 3.0  $\mu\text{m}$ , which acts as 50% output coupler for mid-IR laser output. The residual pump power of a Dy-doped fiber is collimated with an uncoated 20 mm  $\text{CaF}_2$  lens. To separate the mid-IR laser output from the residual pump power an anti-reflection coated Ge filter is used. The mid-IR laser output is recorded as a function of launched pump power and then corrected to subtract the lens and Ge filter loss. This corrected laser output is then used to calculate the laser slope efficiency.

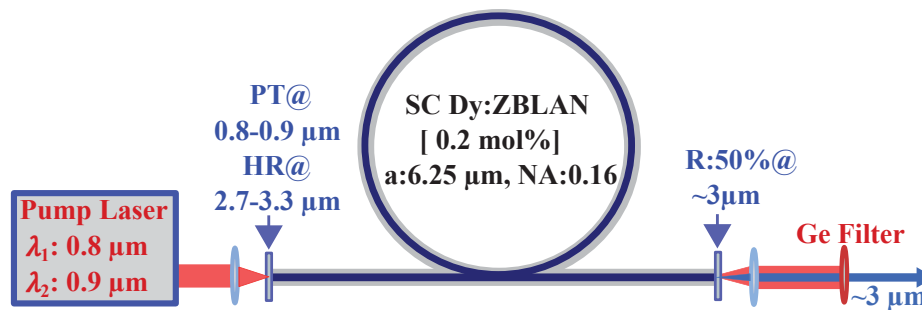


Figure 2. A simple linear cavity Dy-doped ZBLAN mid-IR fiber laser. Two mirrors are butt-coupled with the end faces of the Dy-doped ZBLAN fiber. The front mirror is partially transmissive (PT), 80% at 0.8  $\mu\text{m}$  and 73% at 0.9  $\mu\text{m}$ , for both pump wavelengths and highly reflective (HR), 98% from 2.7–3.2  $\mu\text{m}$ .

## 3. PUMP ABSORPTION ANALYSIS

As both pump wavelengths are below the cut-off wavelength of the Dy-doped fiber, excitation of higher-order modes is expected in the Dy-doped fiber. To observe the higher-order modes excitation in the Dy-doped fiber, we imaged the collimated residual pump power at 0.8  $\mu\text{m}$  by using a Pyrocam IV beam profiling camera. The residual pump power image, as shown in Figure 3. (b), shows the existence of higher-order modes. The excitation of higher-order modes should decrease the pump-core overlap and consequently the effective pump absorption. On the other hand the presence of any unforeseen pump-ESA or any other detrimental higher-order energy transfer mechanism would increase the observed pump absorption. Hence, to understand the effective pump absorption of a Dy ion for both pump wavelengths (0.8  $\mu\text{m}$  and 0.9  $\mu\text{m}$ ), we have measured the residual pump power of a 0.5 m of Dy-doped fiber and compared with numerical simulation data. The pump propagation in the Dy-doped fiber is simulated numerically by solving the system rate equations. To develop a trustworthy numerical model, accurate spectroscopic data input is very important. As the 0.8  $\mu\text{m}$  and 0.9  $\mu\text{m}$  pumping wavelengths are used for the first time in a Dy-doped mid-IR fiber laser, an accurate absorption cross-section data is critical.

For a trustworthy absorption cross-section data of a Dy ion, we have scanned two bulk ZBLAN glass samples doped with 1.0 mol% and 2.0 mol% of dopant concentrations by using a Cary 5000 UV-Vis-NIR spectrophotometer. The recorded data are then post-processed to calculate the Dy ion absorption cross-section by subtracting

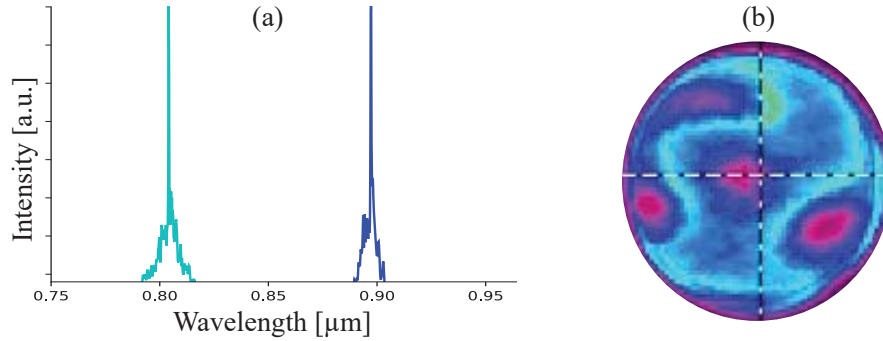


Figure 3. (a) Pump spectrum of a tunable titanium-sapphire laser emitting either at 0.8 μm or 0.9 μm. (b) The residual pump power image (taken by a Pyrocam IV beam profiling camera) shows the higher-order mode excitation at 0.8 μm pumping wavelength.

the background loss of ZBLAN glass. The calculated Dy cross-section, as shown in Figure 4, is used for the numerical simulation of residual pump power.

Comparison of the experimental and the numerical simulation data, as shown in Figure 5(a) and Figure 5(b), show that the experimental residual pump power is higher than the simulated value with 100% pump-core overlap for both pump wavelengths. This resulting from less effective pump absorption in the Dy-doped fiber, which indicate the absence of pump ESA or any higher-order energy transfer mechanism (as expected from the Dy-energy level diagram) for these pumping wavelengths. The less effective pump absorption can then be explained by the fiber multi-mode behaviour at these pumping wavelengths. For the weakly guiding approximations, the number of supported modes that can exist in the Dy-doped fiber for both pumping wavelengths are 10 and 7 for 0.8 μm and 0.9 μm pumping wavelengths, respectively.

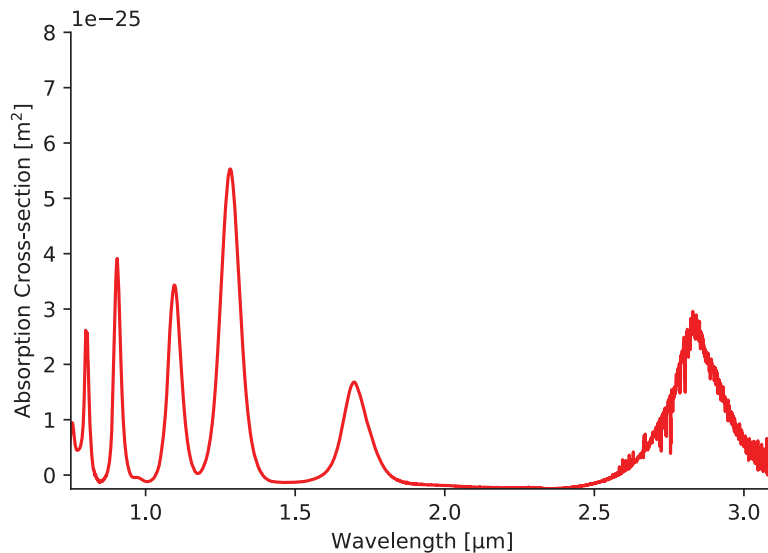


Figure 4. Absorption cross-section of a Dy ion. The absorption cross-section data is measured by using the two bulk ZBLAN glass samples doped with 1.0 mol% and 2.0 mol% of dopant ions.

Due to the multi-mode behaviour of the Dy-doped fiber for these new excitation wavelengths, the pump power confinement in the Dy-doped fiber depends on the degree of excitation of the higher-order modes. We have theoretically calculated the pump power confinement as a function of higher-order modes excitation using

the following relation:<sup>19</sup>

$$\eta = \frac{U^2}{V^2} \left( \frac{W^2}{U^2} + \frac{K_0^2}{K_1^2} \right) \quad (1)$$

where,  $K$ ,  $U = a\sqrt{k_0^2 n_{core}^2 - \beta^2}$ ,  $W = a\sqrt{\beta^2 - k_0^2 n_{clad}^2}$ ,  $V = a\sqrt{k_0^2 n_{core}^2 - k_0^2 n_{clad}^2}$  are modified Bessel function of the second kind, normalised core, cladding, and waveguide parameters, respectively. In the normalized core, cladding, and waveguide parameters;  $a$ ,  $n_{core}$ ,  $n_{clad}$ ,  $k_0 = \frac{2\pi}{\lambda}$ , and  $\beta$  represent the core radius, core-refractive index, cladding-refractive index, propagation constant in free space, and propagation constant of the supported modes, respectively.

Assuming equal excitation of all higher order modes in the Dy-doped fiber, the average pump-power confinement for 0.8  $\mu\text{m}$  and 0.9  $\mu\text{m}$  pump wavelengths are 87.74% and 93%, respectively. To simulate the effect of low pump power confinement in the Dy-doped fiber, the pump-core overlap is varied and experimental results are found in good agreement with the simulation for 87% (for 0.8  $\mu\text{m}$  pumping wavelength) and 91% (for 0.9  $\mu\text{m}$  pumping wavelength) pump-core overlap.

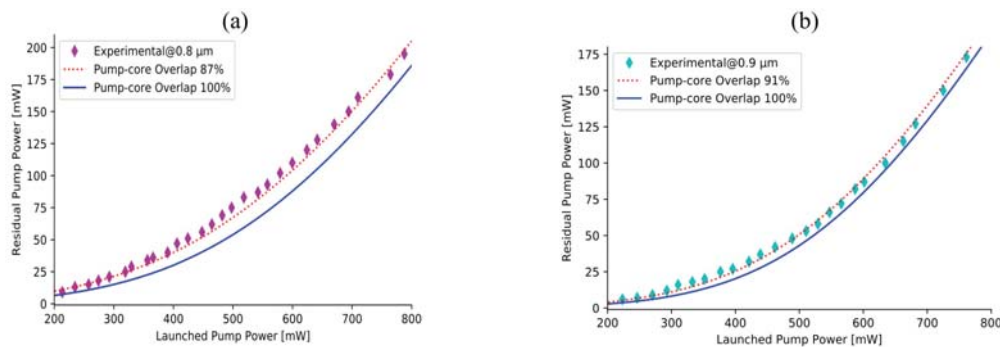


Figure 5. Experimental and numerical residual pump power comparison: (a) for 0.8  $\mu\text{m}$  pumping wavelength, experimental data agree well with simulation data considering 87% pump-core overlap. (b) for 0.9  $\mu\text{m}$  pumping wavelength, 91% pump-core overlap is considered in the numerical model to find good agreement with experimental data.

## 4. RESULTS

The laser slope efficiency as a function of launched pump power is shown in Figure 6(a) for both 0.8  $\mu\text{m}$  and 0.9  $\mu\text{m}$  pumping wavelengths. In our experiment, we have used two different Dy-doped fiber lengths (0.48 m and 0.62 m) as a laser gain medium. The maximum laser slope efficiencies are measured with 0.48 m of Dy-doped fiber, which are 18.5% and 23.7% for 0.8  $\mu\text{m}$  and 0.9  $\mu\text{m}$  pumping wavelength, respectively. When the launched pump power is increased to 449 mW (for 0.8  $\mu\text{m}$  pumping wavelength) and 413 mW (for 0.9  $\mu\text{m}$  pumping wavelength), mid-IR lasing is observed from 0.48 m of Dy-doped fiber. With the increase of Dy-doped fiber length to 0.62 m, the laser slope efficiencies decrease to 17.4% and 22.4% and lasing thresholds increase to 525 mW and 466 mW for 0.8  $\mu\text{m}$ , and 0.9  $\mu\text{m}$  pumping wavelengths, respectively. This investigation indicates the presence of fiber background loss at the signal wavelength. The background loss of this fiber is measured at 3.39  $\mu\text{m}$ , which is 0.3 dB/m<sup>15</sup> and would be similar at  $\sim 3 \mu\text{m}$ . The recorded mid-IR lasing spectra for two different Dy-doped fiber length are shown in Figure 6(b). As the Dy-doped mid-IR fiber laser is a ground state terminated three level system, the signal re-absorption increases in the far end of the fiber (where the fractional population inversion decreases gradually with the increasing fiber length). Consequently, the mid-IR lasing wavelength is shifted towards the longer wavelength region.

To find the relative merit of these new excitation wavelengths, we have compared the performance of all near-IR pumped Dy-doped mid-IR fiber lasers. To date three near-IR excitation wavelengths (1.1  $\mu\text{m}$ ,<sup>11,20</sup> 1.3  $\mu\text{m}$ <sup>13</sup> and 1.7  $\mu\text{m}$ <sup>18</sup>) are used for Dy-doped mid-IR fiber lasers. The maximum laser slope efficiencies are limited to 49%, 38% and 37% of the Stokes limit for 1.1  $\mu\text{m}$ , 1.3  $\mu\text{m}$ , and 1.7  $\mu\text{m}$  excitation wavelengths, respectively. This limited performance is explained by the presence of pump ESA for all these near-IR excitation



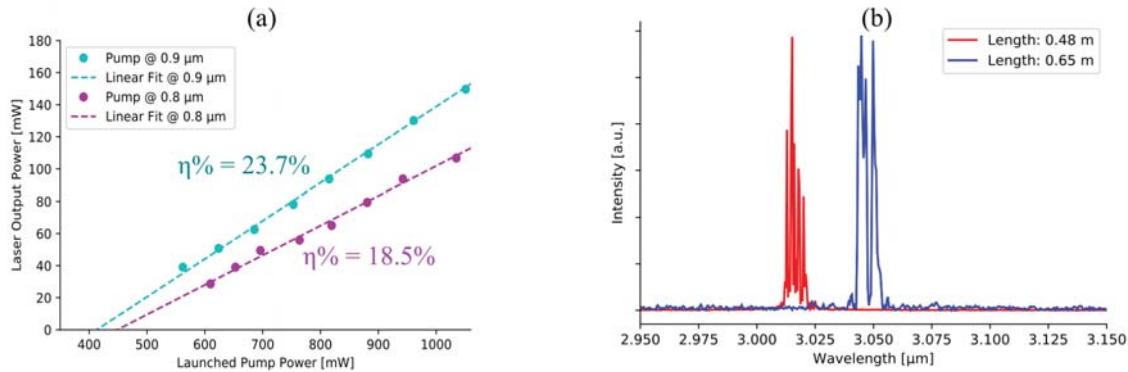


Figure 6. (a) Laser output power as a function launched pump power for 0.48 m of Dy-doped fiber, which produces 18.5% and 23.7% slope efficiency for 0.8 μm and 0.9 μm pumping wavelengths, respectively. (b) The mid-IR laser spectrum as a function of Dy-doped fiber length.

wavelengths. In our current demonstration, we have obtained 70% (at 0.8 μm pumping wavelength) and 79% (at 0.9 μm pumping wavelength) of the stokes limit. This improved performance is obtained due the absence of any detrimental pump-ESA or higher-order energy transfer mechanism for these new excitation wavelengths. These wavelengths can also be used to access the full gain bandwidth of a Dy ion including 4 μm emission, as done in<sup>18</sup> and <sup>7</sup>. The most important feature of these new wavelengths is the availability of the cost-effective high power laser diode.

## 5. CONCLUSION

In conclusion, we have used two new excitation wavelengths (0.8 μm and 0.9 μm) for a Dy-doped mid-IR fiber laser, which are free from detrimental pump ESA or any higher-order energy transfer mechanism. The maximum measured laser slope efficiencies are 18.5% and 23.7% for 0.8 μm and 0.9 μm pumping wavelengths, respectively. The cause of lower slope efficiency than the stokes efficiency limit (70% at 0.8 μm and 79% at 0.9 μm) most likely arises from the fiber background loss (0.3 dB/m measured at 3.39 μm). The commercial existence of the cost effective laser diodes for these new wavelengths open up the possibility to a diode pumped Dy-doped mid-IR fiber laser in a near future.

## ACKNOWLEDGMENTS

This work is supported by funding from the Australian Research Council (ARC DP1700100531) and the US Air Force Asian Office of Aerospace R&D (AOARD FA2386-19-1-0043)

## REFERENCES

- [1] Tittel, F. K., Richter, D., and Fried, A., [*Mid-Infrared Laser Applications in Spectroscopy*], 458–529, Springer Berlin Heidelberg, Berlin, Heidelberg (2003).
- [2] Sijan, A., “Development of military lasers for optical countermeasures in the mid-IR,” in [*Technologies for Optical Countermeasures VI*], **7483**, 748304 (Sept. 2009).
- [3] Woodward, R. I., Majewski, M. R., Hudson, D. D., and Jackson, S. D., “Swept-wavelength mid-infrared fiber laser for real-time ammonia gas sensing,” *APL Photonics* **4**(2), 020801 (2019).
- [4] Adams, A. R., Elliott, C. T., Krier, A., Murdin, B. N., Waynant, R. W., Ilev, I. K., and Gannot, I., “Mid-infrared laser applications in medicine and biology,” *Philosophical Transactions of the Royal Society of London. Series A: Mathematical, Physical and Engineering Sciences* **359**(1780), 635–644 (2001).
- [5] Pereira, M. F., [*Terahertz and Mid Infrared Radiation: Detection of Explosives and CBRN (Using Terahertz) / edited by Mauro F. Pereira, Oleksiy Shulika.*], NATO Science for Peace and Security Series B: Physics and Biophysics (2014).

- [6] Frayssinous, C., Fortin, V., Bérubé, J.-P., Fraser, A., and Vallée, R., “Resonant polymer ablation using a compact 3.44  $\mu\text{m}$  fiber laser,” *Journal of Materials Processing Technology* **252**, 813 – 820 (2018).
- [7] Majewski, M. R., Woodward, R. I., Carreé, J.-Y., Poulain, S., Poulain, M., and Jackson, S. D., “Emission beyond 4  $\mu\text{m}$  and mid-infrared lasing in a dysprosium-doped indium fluoride ( $\text{InF}_3$ ) fiber,” *Optics Letters* **43**, 1926–1929 (Apr 2018).
- [8] Auzel, F., Meichenin, D., and Poignant, H., “Laser cross-section and quantum yield of  $\text{Er}^{3+}$  at 2.7  $\mu\text{m}$  in a  $\text{ZrF}_4$ -based fluoride glass,” *Electronics Letters* **24**, 909–910 (July 1988).
- [9] Henderson-Sapir, O., Jackson, S. D., and Ottaway, D. J., “Versatile and widely tunable mid-infrared erbium doped ZBLAN fiber laser,” *Optics Letters* **41**, 1676–1679 (Apr 2016).
- [10] Crawford, S., Hudson, D. D., and Jackson, S. D., “High-power broadly tunable 3- $\mu\text{m}$  fiber laser for the measurement of optical fiber loss,” *IEEE Photonics Journal* **7**, 1–9 (June 2015).
- [11] Jackson, S. D., “Continuous wave 2.9  $\mu\text{m}$  dysprosium-doped fluoride fiber laser,” *Applied Physics Letters* **83**(7), 1316–1318 (2003).
- [12] Tsang, Y. and El-Taher, A., “Efficient lasing at near 3  $\mu\text{m}$  by a Dy-doped ZBLAN fiber laser pumped at 1.1  $\mu\text{m}$  by an Yb fiber laser,” *Laser Physics Letters* **8**(11), 818–822.
- [13] Tsang, Y. H., El-Taher, A. E., King, T. A., and Jackson, S. D., “Efficient 2.96  $\mu\text{m}$  dysprosium-doped fluoride fibre laser pumped with a Nd:YAG laser operating at 1.3  $\mu\text{m}$ ,” *Optics Express* **14**, 678–685 (Jan 2006).
- [14] Majewski, M. R. and Jackson, S. D., “Highly efficient mid-infrared dysprosium fiber laser,” *Optics Letters* **41**, 2173–2176 (May 2016).
- [15] Woodward, R. I., Majewski, M. R., Bharathan, G., Hudson, D. D., Fuerbach, A., and Jackson, S. D., “Watt-level dysprosium fiber laser at 3.15  $\mu\text{m}$  with 73% slope efficiency,” *Optics Letters* **43**, 1471–1474 (Apr 2018).
- [16] Fortin, V., Jobin, F., Larose, M., Bernier, M., and Vallée, R., “10-W-level monolithic dysprosium-doped fiber laser at 3.24  $\mu\text{m}$ ,” *Optics Letters* **44**, 491–494 (Feb 2019).
- [17] Majewski, M. R. and Jackson, S. D., “Tunable dysprosium laser,” *Opt. Lett.* **41**, 4496–4498 (Oct 2016).
- [18] Majewski, M. R., Woodward, R. I., and Jackson, S. D., “Dysprosium-doped ZBLAN fiber laser tunable from 2.8  $\mu\text{m}$  to 3.4  $\mu\text{m}$ , pumped at 1.7  $\mu\text{m}$ ,” *Optics Letters* **43**, 971–974 (Mar 2018).
- [19] Digonnet, M. J. F. and Gaeta, C. J., “Theoretical analysis of optical fiber laser amplifiers and oscillators,” *Applied Optics* **24**, 333–342 (Feb 1985).
- [20] Sójka, L., Pajewski, L., Popenka, M., Beres-Pawlik, E., Lamrini, S., Markowski, K., Osuch, T., Benson, T. M., Seddon, A. B., and Sujecki, S., “Experimental investigation of mid-infrared laser action from  $\text{Dy}^{3+}$ -doped fluorozirconate fiber,” *IEEE Photonics Technology Letters* **30**, 1083–1086 (June 2018).